THEORETICAL BACKGROUND FOR THE FATIGUE CRACKS KINETICS SIMULATION

N. V. Tumanov*

Using the experimental results obtained earlier, the Author has developed a crack kinetics model based on the interpretation of the consecutive qualitative changes of the material properties at the crack's apex which are caused by a local evolution of the defects' structure (dislocations, vacancies, and micropores). A qualitative mathematical model of the crack kinetics has been proposed, in whose framework the system "propagating crack - material at its front" (the CM-system) is considered as a non-linear dynamic system with a parametric action. Its analysis under a quasi-static and random action makes it possible to describe qualitatively on a common basis the peculiarities of the fatigue cracks kinetics under regular and irregular loading.

INTRODUCTION

The experimental dependence which connects the crack propagation velocity $V = dl / dN$ (l is the crack length, N is the number of cycles) with the envelope K_e of the stresses intensity coefficient K, varying quasi-statically, is the most widespread equation of the fatigue crack kinetics (for a symmetrical loading cycle). Its diagram (the kinetic diagram of fatigue failure (KDFF)) is shown schematically in Fig. 1. It is obvious that the revealed behaviour of the crack kinetics (Tumanov and Cherkasova (1)) cannot be described by an algebraic constraint between V and K_e. The idea propounded in the present paper is based on using the results (1) for interpreting the successive changes of the material properties at the fatigue crack apex, which have been caused by a local evolution of a defects' structure, developing in stages after the threshold stresses levels have been exceeded (Kulemin (2)).

Physical model. In conformity with the suggested idea, the first KDFF section (Fig.1) corresponds to the pre-threshold stresses level at the crack apex. On the second KDFF section the stresses level at the crack front exceeds the first threshold value (the value K_{el-2} corresponds to it), which causes an activation of dislocation sources and a simultaneous increase of the vacancies concentration (2). Fractographically, this is evidenced by fatigue

* Central Institute of Aviation Motors, Moscow

striations which are formed as a result of the collectivised dislocations output on to the fracture surface ((1), Fig.2a); and physically this is evidenced by an increase of hardness (due to the increase of the slowed-down dislocations density) and a decrease of the material density at the crack apex. This leads to the formation of a strengthened and extended layer over there, in which a cyclic plastic deformation of a constant sign (with a positive asymmetry coefficient) is implemented, and which prevents the crack closure and hinders its growth (the value $\partial V/\partial K$ is sharply diminished as compared to the first section).

The K_e increase within the second KDFF section causes a multiple (turbulent) slippage at the crack apex and an activation of the dislocations creeping-over, which is a result of the satiation with vacancies. As a result, the slippage lines and the fatigue striations formed by them acquire a torn and devious nature ((1), Fig.2d). With the further K_e increase, an opposite trend starts to develop at the crack front along with strengthening: due to the condensation of vacancies and appearance of microfractures in the places of the accumulation of slowed-down dislocations the number of micropores grows, the dislocation accumulations are discharged, and the density of mobile dislocations increases, that is, de-strengthening (loosening) of the material takes place. These changes lead to the appearance of a new micromechanism of destruction, namely, shearing of partitions between the micropores followed by the formation of a dimpled microrelief of the fracture. For $K_e > K_{e2\text{-}3}$ the indicated mechanism becomes determining; a loosened layer of material is formed at the crack front and its velocity grows abruptly.

The nature of the dependence between K_e and the microhardness H of the material at the crack front, which is indicative of the above behaviour, is shown in Fig.2. Since the velocity of the defects' structure evolution under a cyclic action increase with the growth of the stresses level (2), then the material located in front of the crack front is at different stages of this evolution. The latest stage is observed at the crack front, and further on with the growing distance from the crack all previous stages are implemented. Accordingly, the properties of the material and its states are changing (Fig.2). For $K_e > K_{e2\text{-}3}$ the loosened layer at the crack front is followed by a layer of the material whose state directly precedes loosening, i.e., the maximum strengthened and extended layer. The presence of this layer 1) prevents the crack closure, providing an intact plastic microrelief (dimples) under considerable compressive overloads, and 2) localises the material plastification at the crack front, due to which the plastic microrelief is combined with the microbrittle fracture (1).

To formalise the above described phenomena, it has been found advantageous to introduce a notion of the "propagating crack - material at its front" system (CM-systems) whose state is characterised by the crack propagation velocity V and the microhardness H of the material at its front; the controlling variable is the value of K_e, and the diagrams "V-K_e" and "H-K_e" in Figs. 1 and 2 (obtained under the condition that the typical time τ_T of the K_e variation is much greater than the relaxation time τ_R of the CM-system to its equilibrium states) are diagrams of the equilibrium states of the CM-system. Therefore, the values $V_{2\text{-}3}$, $H_{2\text{-}3}$ and $K_{e2\text{-}3}$ on these diagrams determine the critical point of the CM-system which corresponds to the bifurcation of its equilibrium states or to the equilibrium phase transition from a strengthened state into a loosened state (to the SL-transition), whose fractographical feature is a smooth (through the mixed relief area) striated-dimpled transition of the microrelief. In this context the anomalous scatter of the striations pitch in

the extended area of the mixed dimpled-striated relief (1) is a typical critical phenomenon - anomalous fluctuations of the system's state variables near the critical point. Since the transition is equilibrium, it is completely inverse, which can be seen from the nature of the change of the fracture microrelief (1).

For a fast variation of K_e ($\tau_T << \tau_R$) (in particular, in case of random fluctuations of K_e with the correlation time $\tau_C << \tau_R$ implemented in the basic experiment (1)), the state of the CM-system is determined by the mean value of the controlling parameter everywhere, except the area adjacent to its bifurcation values. Fluctuations of K_e in the vicinity of $K_{e2\text{-}3}$ lead to non-equilibrium phase SL- and LS- transitions of the CM-system - a transition from the strengthened state into a loosened one and back beyond the critical point. A peculiarity of these transitions is their abrupt spasmodic nature, since the CM-system slips by the intermediate states or maintains them for a long time. Under non-equilibrium conditions in the vicinity of the bifurcation value of the controlling parameter, the CM-system functions on two temporal scales: the stay in each state is followed by an abrupt transition between them, i.e., a bistable condition is implemented which causes a spasmodic crack kinetics. The fractographic indications of such behaviour are fatigue bands and spasmodic dimpled-striated and striated-dimpled transitions of the fracture microrelief (DS- and SD-transitions) (1).

Mathematical model. We consider the following dynamic system as the simplest qualitative model of the CM-system: $\dot{V} = \varphi_\lambda(V)$, here λ is the controlling parameter, and $\varphi_\lambda(V)$ is the function which is non-linear in relation to V and linear in relation to λ. Expanding it into a series with respect to the equilibrium values of the crack propagation velocity V_1, which correspond to the strengthened state of the CM-system (the second KDFF section), and, restricting ourselves to the first two terms, we obtain $\dot{x} = a_1 x + a_2 x^2$, where $x = V - V_1$. Let $a_1 = a\lambda$ $(a > 0)$, where $\lambda = (K_e - K_{e2\text{-}3}) / K_{e2\text{-}3}$. Introducing the dimensionless time $\tau = at$, we obtain

$$\dot{x} = \lambda x - cx^2, \qquad (1)$$

where $c = -a_2 / a$ $(a_2 < 0)$. The bifurcation diagram of the stationary solutions of Eq.(1) is given in Fig.3 (the solid lines correspond to the stable states, the dashed lines - to the unstable ones). The signs of a_1 and a_2 have been chosen so, that the velocity in the super-critical state $V_2 = V_1 + \lambda / c$ (the third KDFF section) exceeded the sub-critical velocity V_1, the way this happens under the SL-transition of the CM-system. As is evident, the bifurcation diagram provides a qualitatively proper reflection of the KDFF behaviour in the vicinity of $K_{e2\text{-}3}$.

To analyse the non-equilibrium states of the CM-system, we consider the solutions of Eq.(1) under the conditions of fast random fluctuations of the controlling parameter λ (relative to the mean value $\bar{\lambda} = (\bar{K}_e - K_{e2-3}) / K_{e2-3}$, where $\bar{K}_e$ is the mean value of K_e). We assume that $\tau_C << \bar{\lambda}^{-1}$, this makes it possible to employ the Markov processes method. The Fokker-Plank-Kolmogorov equation for the unidimensional density of the system's state probability $p(x,t)$ has the form

$$\frac{\partial p(x,t)}{\partial t} = -\frac{\partial}{\partial x}\left\{\left[(\gamma-1)x - cx^2 + \frac{\gamma^2 v_K^2}{2}\right]p(x,t)\right\} + \frac{\gamma^2 v_K^2}{2}\frac{\partial^2 x^2 p(x,t)}{\partial x^2}, \quad (2)$$

where $\gamma = \overline{K}_e / K_{e\,2\text{-}3}$, $v_K = \sigma_K / \overline{K}_e$ is the variation coefficient K_e , σ_K is its root-mean-square deviation. For $\gamma > 1$ Eq.(2) has a stationary solution $p_S(x)$ - gamma-distribution with parameters $\alpha = 2(\gamma-1)/\gamma^2 v_K^2$, $\beta = 2cK_{e2-3}^2 / \sigma_K^2$. For $\gamma < 1$ there exists a single stationary state $x = 0$, i.e., $p_S(x) = \delta(x)$, where $\delta(x)$ is the delta-function. As can be seen from Fig.4, for $\gamma < 1$ the system is in the sub-critical non-equilibrium state $(x = 0)$; for $\gamma > 1$ and $\alpha > 1$ it is in the super-critical state $(x > 0)$; and for $0 < \alpha \leq 1$ both states are possible, that is, the system is in the bi-stability condition. The bifurcation diagram of the stationary non-equilibrium states of the CM-system, which characterises the qualitative change of $p_S(x)$ depending on the parameters γ and v_K , is shown in Fig.5. In conformity with the experimental data revealed in (1), the bi-stability condition, which is absent under the equilibrium conditions $(v_K = 0)$, is located between the sub- and super-critical non-equilibrium states, and with the increase of γ the CM-system passes consecutively from the sub-critical state into the bi-stability condition, and afterwards into the sup-critical state.

Adequacy check. In addition to the qualitative agreement with the regularities which were revealed early, the suggested model has predicted one more regularity, namely, the expansion of the bi-stability area with the growth of v_K (Fig.6), which has been confirmed by a special experiment. As can be seen from Fig.6, the fracture section with fatigue bands corresponding to the bi-stable behaviour of the CM-system (to the spasmodic crack kinetics) increases consecutively with the growth of v_K .

REFERENCES

(1) N.V.Tumanov and S.A.Cherkasova, Experimental Background for the Fatigue Cracks Kinetics Simulation. In the present collection of papers.

(2) A.V.Kulemin, Ultra-Sound and Diffusion in Metals, Metallurgy, Moscow, 1978.

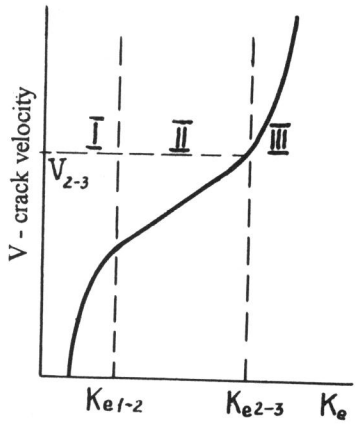

Fig. 1 The kinetic diagram of the fatigue failure.

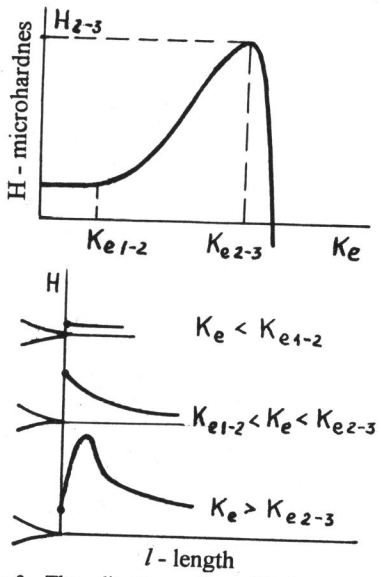

Fig.2 The diagram of equilibrium states "H - K_e " and modification of the material properties in front of the crack's front.

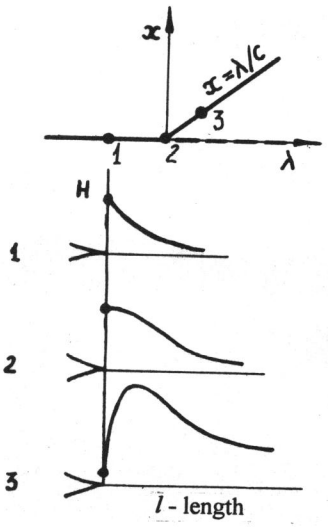

Fig.3 The bifurcation diagram of the equilibrium states of the CM-system model.

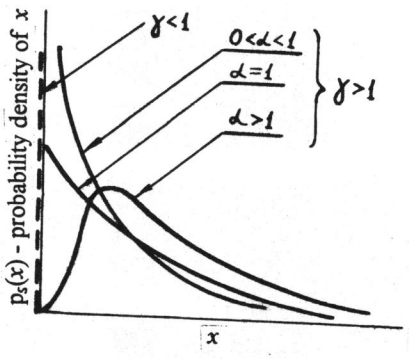

Fig. 4 The probability density of the stationary non-equilibrium states of the CM-system model.

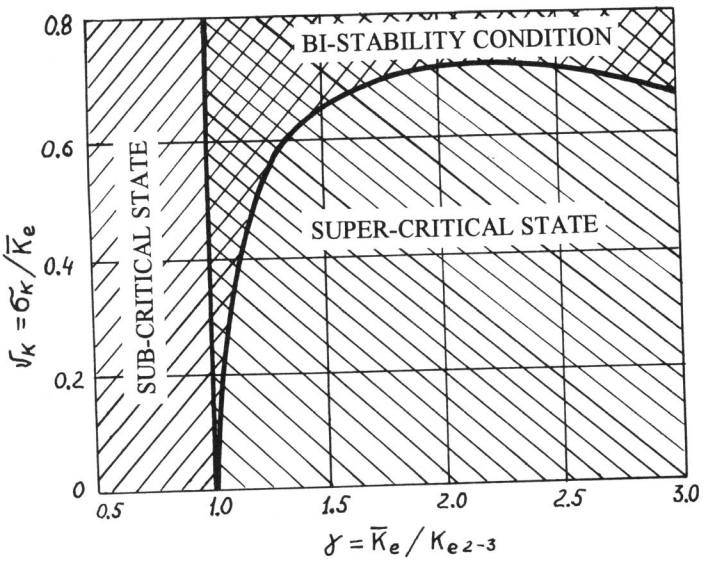

Fig. 5 The bifurcation diagram of the stationary non-equilibrium states of the CM-system model.

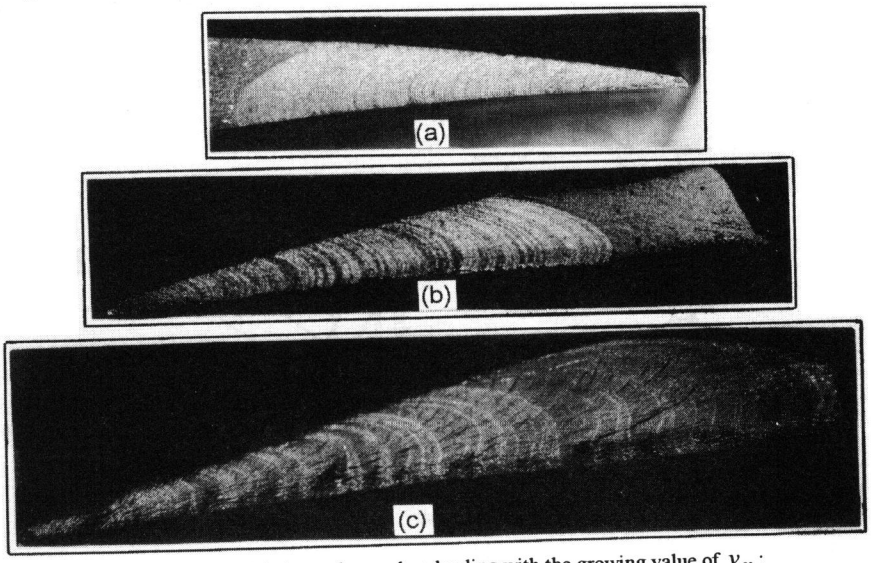

Fig. 6 Fatigue fractures of blades under random loading with the growing value of ν_K :
(a) $\nu_K = 0.1$, (b) $\nu_K = 0.3$, (c) $\nu_K = 0.4$.